

Keap1/Nrf2 Signaling Regulates Oxidative Stress

Tolerance and Lifespan in *Drosophila*

Gerasimos P. Sykiotis and Dirk Bohmann

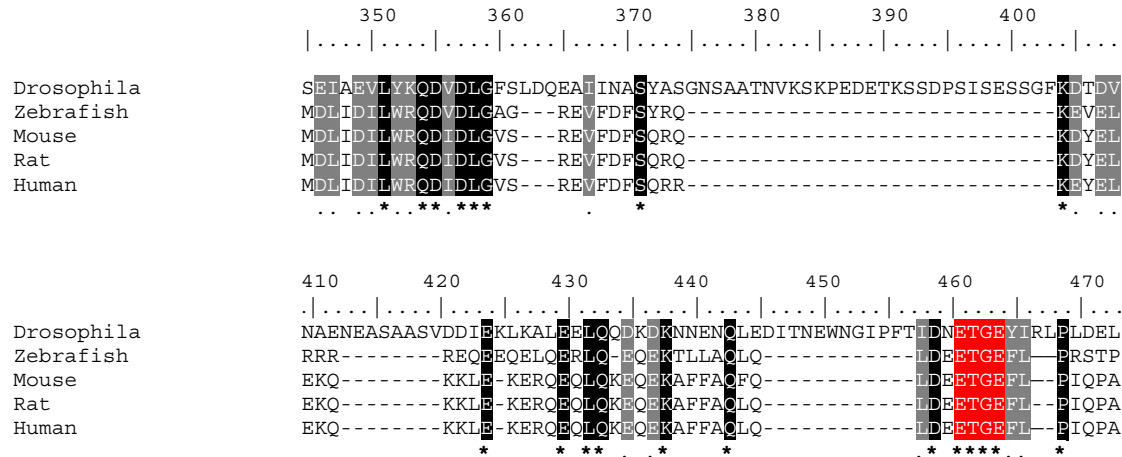


Figure S1A. *Drosophila* CncC Contains a Peptide Sequence with Similarity to the Keap1 Binding Motifs of Vertebrate Nrf2 Proteins

An ETGE motif (highlighted in red) and an upstream hydrophobic segment characteristic of Keap1-binding Nrf2 Neh2 domains are conserved in CncC. Protein Accession numbers of the aligned proteins are: NP_732833.1 (*Drosophila*), NP_878309.1 (zebrafish), NP_057888.1 (mouse), NP_113977.1 (rat), and NP_006155.2 (human).

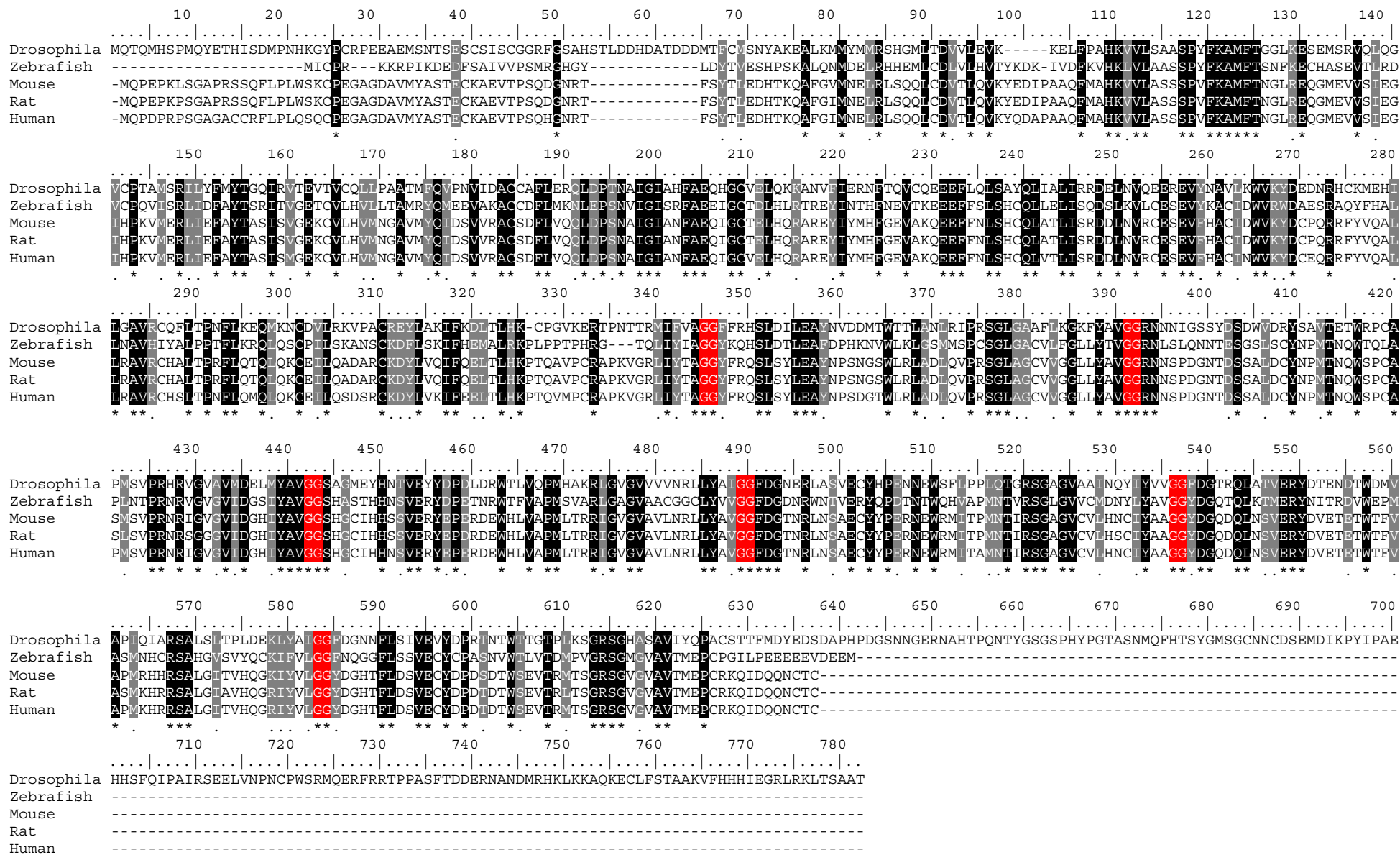


Figure S1B. *Drosophila* Keap1 Is Highly Homologous to Its Zebrafish and Mammalian Homologs (e.g., 38.1% Identical to Human Keap1)

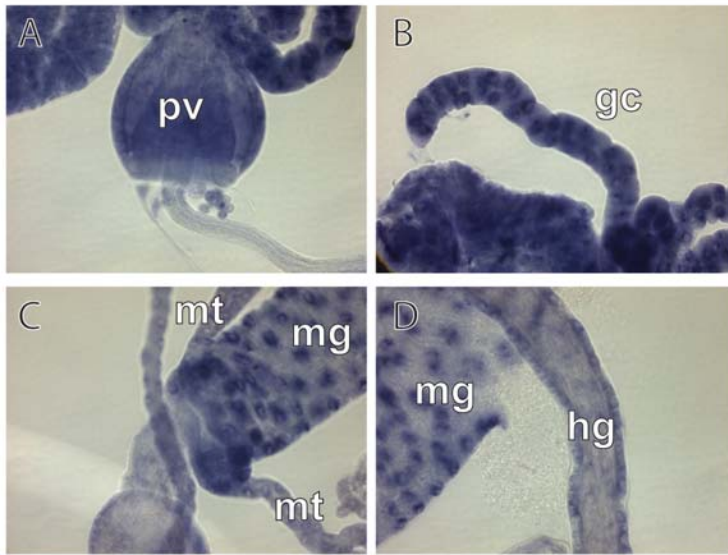
The multiple sequence alignment was constructed using ClustalW, and annotated using Boxshade (www.ch.embnet.org/software/BOX_form.html):

identical amino acids are denoted by black shading and the “*” sign, similarity is denoted by gray shading and the “.” sign. The NCBI Protein

Accession numbers of the aligned proteins are: NP_650594.1 (*Drosophila*), NP_878284.2 (zebrafish), NP_057888.1 (mouse), NP_476493.1 (rat), and

NP_036421.2 (human). The six double-glycine repeats (highlighted in red) are key structural features of the Kelch domains.

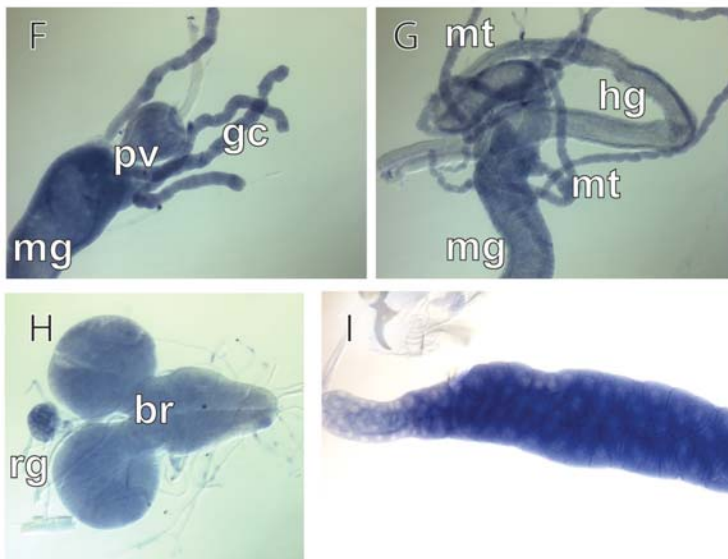
cncC



cncC in situ hybridization

- A proventriculus (pv)
- B gastric caeca (gc)
- C posterior midgut (mg) and malpighian tubules (mt)
- D posterior midgut (mg) and hindgut (hg)
- E salivary gland

keap1



keap1 in situ hybridization

- F proventriculus (pv), gastric caeca (gc), and anterior midgut (mg)
- G posterior midgut (mg), hindgut (hg), and malpighian tubules (mt)
- H brain (br) and ring gland (rg)
- I salivary gland

Figure S2. *Drosophila cncC* and *keap1* Are Expressed in Multiple Organs

The expression of the *cncC* and *dkeap1* genes was analyzed in third instar larvae by *in situ* mRNA hybridization. The *cncC* hybridization probe was specific for the *cncC* transcript (it did not recognize the *cncA* and *cncB* isoforms). Both *cncC* and *dkeap1* showed broad expression in the alimentary canal and in other organs that are expected to be exposed to oxidative stress or to be sensitive to such stress. *cncC* is expressed in a strong, distinctive pattern in the proventriculus and gastric caeca, in most parts of the midgut, and in the hindgut. It is also expressed in the

Malpighian tubules and the salivary glands. The expression pattern of *keap1* largely follows that of *cncC* in its topology, but it is not as pronounced. Marked *keap1* expression is also seen in the brain and the adjacent ring gland. Note that removal of *keap1* function in clones of brain tissue causes increased CncC reporter activity (see Figure S4D).

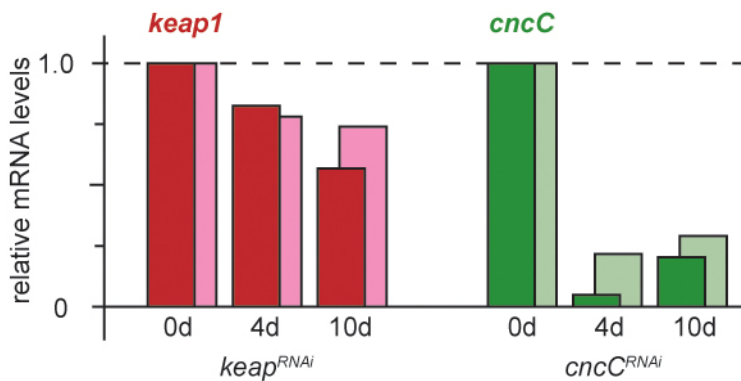


Figure S3. *UAS cncC^{RNAi}* and *UAS keap1^{RNAi}* Effectively Knock Down Their mRNA Targets in Adult Flies

UAS constructs for hairpin RNAs that give rise to RNAi targeting, respectively, *cncC* and *keap1* were expressed under the control of RU486 using *tubGS5* (dark red and dark green bars) or *tubGS10* (light red and light green). The expression of *UAS keap1^{RNAi}* or *UAS cncC^{RNAi}* (indicated at the bottom of the histogram) was activated by feeding adults with RU486 as detailed in the methods section. Genetically identical siblings from the same culture were treated with control food not containing the drug. The resultant changes in the mRNA levels of *cncC* and *keap1* were examined by real time RT-PCR after 4 and 10 days of conditional knockdown.

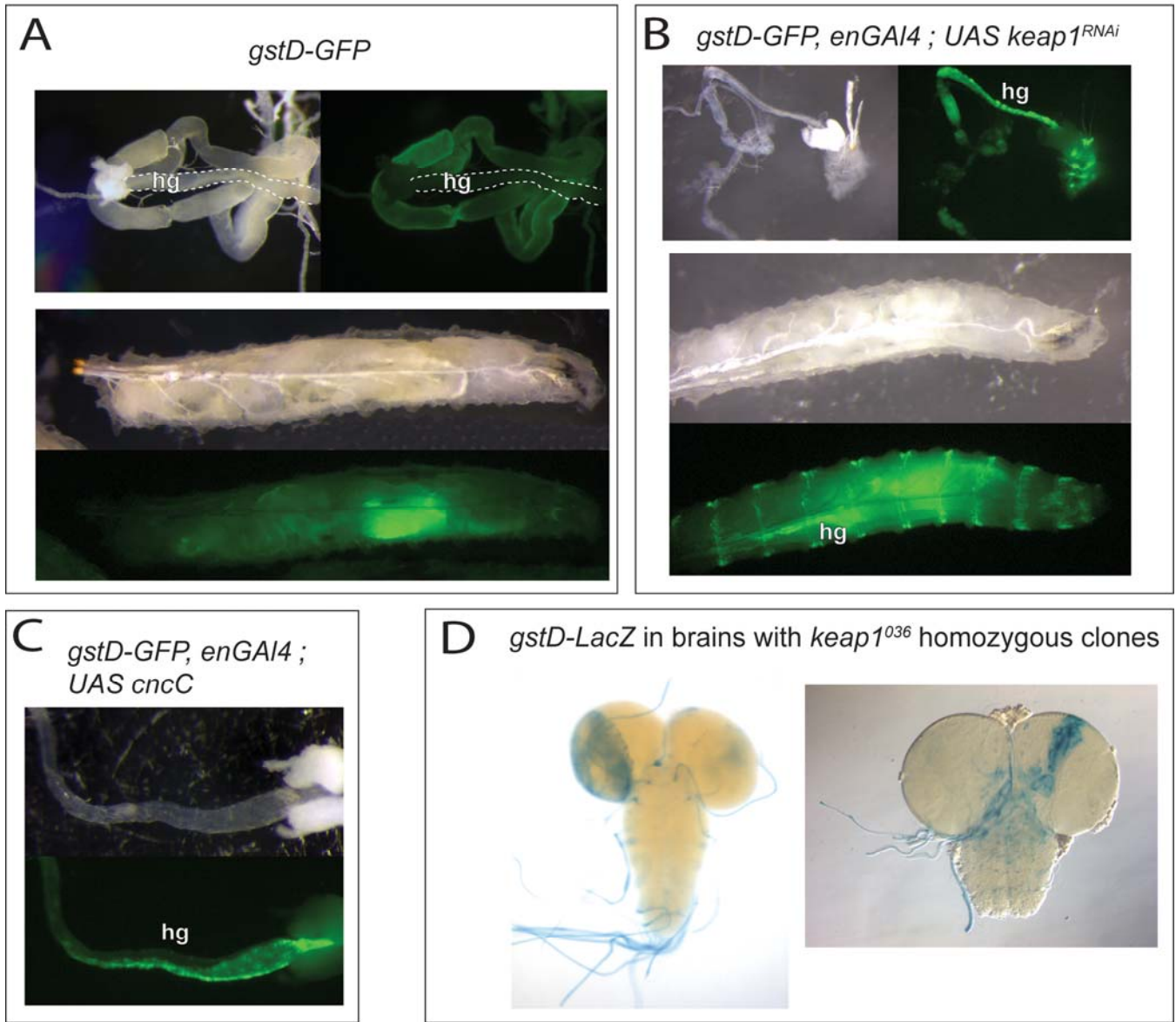


Figure S4. Suppression of Keap1 Expression Stimulates the Cnc Reporter in Multiple Tissues

A. Expression of the CncC-responsive *gstD-GFP* reporter in wild type larvae. Specimens are shown in white light or under UV to reveal areas of reporter activity. Note that under these normal conditions the reporter is predominantly expressed in the gut. Inspection of the dissected

larval intestine (top panels) shows prominent reporter activity in the foregut and midgut, but no detectable fluorescence in the hindgut (hg, dashed outline).

B. Same analysis as in A, except in a larva in which *UAS keap1^{RNAi}* is expressed under the control of the *enGal4* driver. Note the clear expression of the CncC reporter in the characteristic *engrailed* pattern in the epidermis and the hindgut (hg).

C. Expression of CncC under the control of *enGal4* causes activation of the reporter in the hindgut in a manner that is comparable to the effect of *keap1^{RNAi}*. Induction in the epidermis was also observed (not shown).

D. Brains harboring homozygous mutant clones of the *keap1⁰³⁶* allele show activation of the *gstD-lacZ* reporter.

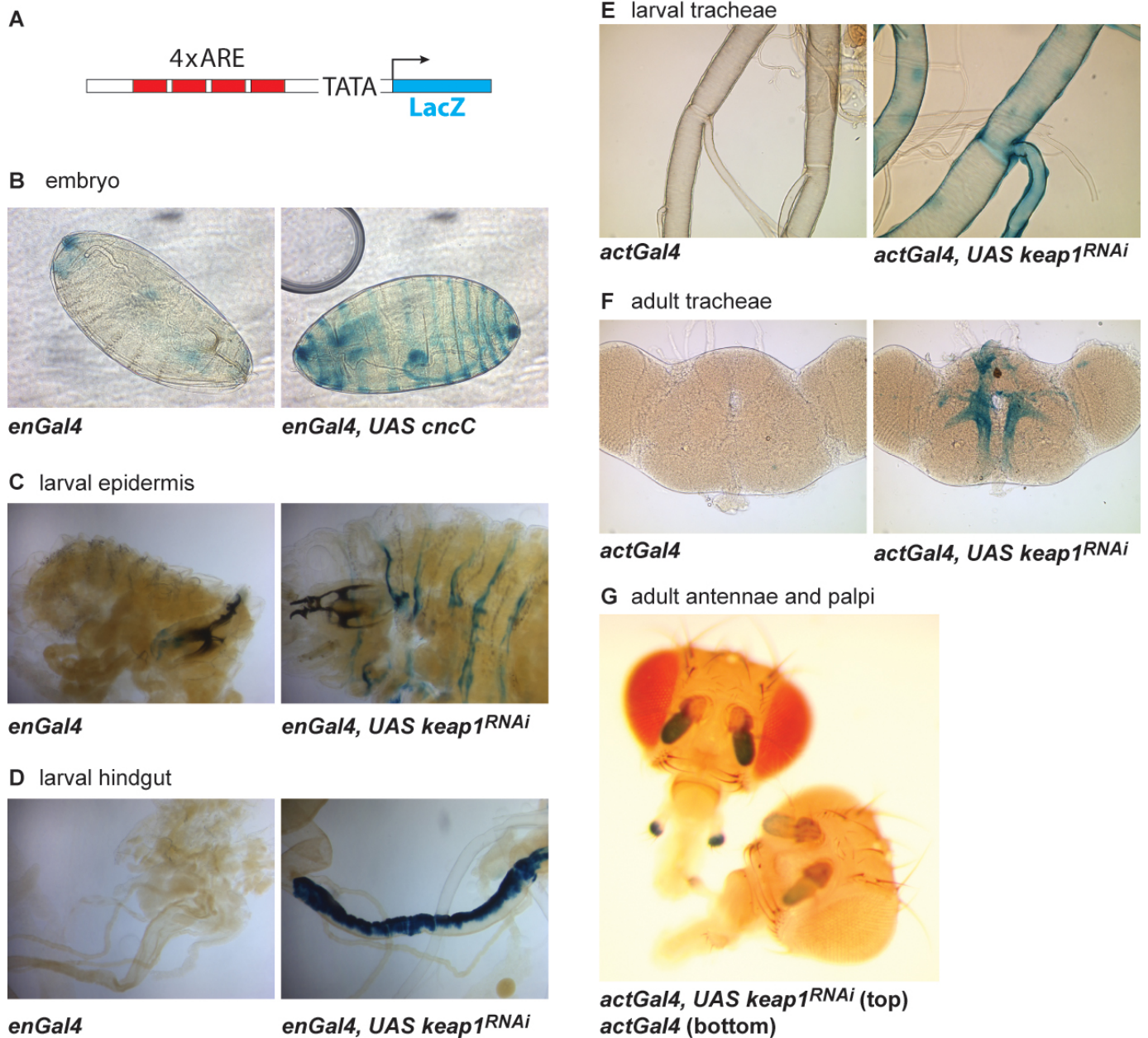


Figure S5. The ARE Is Sufficient for In Vivo Transcriptional Activation by Keap1/CncC

A. A multimer ARE-lacZ reporter transgene was used to assay ARE-mediated transcriptional activity. The cloned ARE (TGACTCAGC) was previously identified as a sequence that binds the CncB isoform, which is entirely contained within CncC.

B. In *Drosophila* embryos that carry the 4xARE-lacZ reporter, CncC was over-expressed using the *enGal4* driver. X-gal staining of these embryos reveals a pattern of lacZ expression in the epidermis and dorsal hindgut that corresponds to the areas of *enGal4* activity.

C-D. In third instar larvae expressing *UAS keap1^{RNAi}* under the control of *enGal4*, induction of lacZ activity is observed in the epidermis (C), and in the dorsal hindgut (D).

E-F. Expression of *UAS keap1^{RNAi}* under the control of *act5CGal4* induces lacZ activity in the larval (E) and adult (F) trachea, and in the adult antennae and maxillary palpi (G).

Supplemental Experimental Procedures

Generation of *keap1* Mutations

The P-element *EY02632* is a homozygous viable insertion in the *keap1* locus that does not reside in a coding region. We mobilized *EY02632* by crossing with a *P{ry[+t7.2]=Delta2-3}99B* transposase stock, and generated a deletion of 1500 bp that encompasses the translation start site, *keap1⁰³⁶* (Figure 6A). The *keap1⁰³⁶* allele is lethal at larval stages when homozygous or when trans-heterozygous with deficiency *Df(3R)Exel6176*, which uncovers the *dkeap1* locus.

Expressing Keap1 from a UAS transgene using the ubiquitous *armadilloGal4* or *tubulinGal4* driver in these trans-heterozygous mutants can rescue the flies to adulthood. Although *keap1⁰³⁶* behaves as a null allele, it is not suitable for analyses of oxidative stress resistance and lifespan, because it is unmarked and cannot be easily tracked during backcrossing into a specific genetic background, thus precluding comparisons of otherwise genetically identical flies. Therefore, we next mobilized the original *EY02632* P-element again and selected flies with potential new P-element insertions (darker eye color) that did not complement the *keap1⁰³⁶* deletion. Two new insertions in the *keap1* locus were isolated in independent rounds of mutagenesis: *keap1^{EY1}* and *keap1^{EY5}*, Figure 6A. Mapping the insertion sites by a standard inverse PCR protocol showed that the *keap1^{EY1}* and *keap1^{EY5}* insertions disrupt coding exons of the *keap1* gene. *keap1^{EY1}* and *keap1^{EY5}* are larval lethal when trans-heterozygous with *keap1⁰³⁶*, with *Df(3R)Exel6176*, or with each other (they retained these properties after extensive backcrossing into a *w¹¹¹⁸* background).

These alleles are marked by *mini-white* transgenes, which facilitated the backcrossing of each allele into a w^{1118} genetic background. More than 12 backcrosses were performed, after which the two backcrossed *keap1* lines were out-crossed to an independent white stock (y^l, w^{1118}). The oxidative stress tolerance and lifespan of heterozygous mutant and wild-type progeny of this cross were compared.

Table S1. Paraquat Resistance and Longevity Assays on *keap1* Heterozygotes

Genotype	Mean % Survival (±Standard Error)	Number of Cohorts	Total Number of Flies	p Value for Difference (2-tailed)
♂ <i>keap1^{EY1}/+</i>	64.53 ± 4.60	10	1085	<0.001
♂ +/+	46.83 ± 3.93	10	1051	
♂ <i>keap1^{EY5}/+</i>	59.60 ± 4.86	10	1264	<0.005
♂ +/+	45.49 ± 5.87	10	1087	
♀ <i>keap1^{EY1}/+</i>	52.43 ± 3.00	9	1195	=0.24
♀ +/+	48.61 ± 3.32	9	1220	
♀ <i>keap1^{EY5}/+</i>	42.38 ± 3.14	9	1068	=0.41
♀ +/+	43.34 ± 3.52	9	1081	

Genotype	Mean Lifespan (±Standard Error)	95% Confidence Interval	Median Lifespan (±Standard Error)	95% Confidence Interval	Number of Independent Cohorts	Total Number of Flies
♂ <i>keap1^{EY1}/+</i>	59.16 ± 0.31	58.56 – 59.76	60.00 ± 0.22	59.57 – 60.43	4	699
♂ +/+	54.80 ± 0.34	54.13 – 55.47	56.00 ± 0.44	55.14 – 56.86	4	665
♂ <i>keap1^{EY5}/+</i>	61.17 ± 0.37	60.44 – 61.89	63.00 ± 0.13	62.75 – 63.25	3	509
♂ +/+	55.41 ± 0.35	54.73 – 56.09	58.00 ± 0.14	57.20 – 58.28	3	490

The top panel shows the results of the Paraquat tolerance assays for male and female *keap1^{EY1}* and *keap1^{EY5}* flies and their sibling controls. The bottom panel shows the results of the longevity assays for the male flies.